Am J Physiol Cell Physiol 311: C1040–C1047, 2016.
First published October 26, 2016; doi:10.1152/ajpcell.00211.2016.

Monitoring of ovarian cancer cell invasion in real time with frequency-dependent impedance measurement

Chun-Min Lo,[1] Jun-Chih Lo,[2] Priscila Y. Sato,[3] Tsz-Lun Yeung,[4] Samuel C. Mok,[4] and Kay-Pong Yip[5]

[1]*Department of Biomedical Engineering, National Yang-Ming University, Taipei, Taiwan;* [2]*Graduate Institute of Natural Healing Sciences, Nanhua University, Chia-Yi, Taiwan;* [3]*Center for Translational Medicine, Temple University School of Medicine, Philadelphia, Pennsylvania;* [4]*Department of Gynecologic Oncology and Reproductive Medicine, The University of Texas MD Anderson Cancer Center, Houston, Texas; and* [5]*Department of Molecular Pharmacology and Physiology, University of South Florida, Tampa, Florida*

Submitted 19 July 2016; accepted in final form 18 October 2016

Lo CM, Lo JC, Sato PY, Yeung TL, Mok SC, Yip KP. Monitoring of ovarian cancer cell invasion in real time with frequency-dependent impedance measurement. *Am J Physiol Cell Physiol* 311: C1040–C1047, 2016. First published October 26, 2016; doi:10.1152/ajpcell.00211.2016.—The conventional approach to assessing cancer invasion is primarily for end-point analysis, which does not provide temporal information on the invasion process or any information on the interactions between invading cells and the underlying adherent cells. To alleviate these limitations, the present study exploited electric cell-substrate impedance sensing (ECIS) to monitor the invasion of ovarian cancer cells (SKOV-3) through an adherent monolayer of human umbilical vein endothelial cells (HUVECs). Impedance was measured at 4 kHz of AC voltage or was measured as a function of AC frequency (25 Hz to 60 kHz). By measuring impedance at 4-kHz AC, we found that the invasion of SKOV-3 cells through the HUVEC monolayer was manifested as a rapid decrease in transendothelial electrical resistance in real time. The invasion was augmented in the presence of hepatocyte growth factor (HGF). The enhancing effect of HGF was attenuated by c-Met inhibitor (SU11274). By measuring the frequency-dependent impedance of SKOV-3 cells over time, we found that HGF-enhanced SKOV-3 cell invasion was accomplished with reduced junctional resistance (R_b), increased average cell-substrate separation (h), and increased micromotion. SU11274 attenuated the effects of HGF on R_b, h, and micromotion in the SKOV-3 monolayer. SU11274 also increased the barrier function of the HUVEC monolayer by increasing R_b and decreasing h. In conclusion, this study demonstrated an improved method for monitoring and studying the interactions between cancer cells and the underlying adherent cells during invasion in real time. Alterations in cellular biophysical properties (R_b, h) associated with cancer transendothelial invasion were detected.

electric cell-substrate impedance sensing; c-Met; hepatocyte growth factor; ovarian cancer

ADVANCED OVARIAN CANCER (OVCA) accounts for most of the ~20,000 new cases of epithelial OVCA each year in the United States. More than 16,000 patients die of OVCA each year, making this cancer the most lethal gynecologic malignancy. Although a subset of patients survive more than 5 yr, cancer recurs in the vast majority of patients within 12–24 mo after diagnosis, and these patients die of recurrent metastatic diseases. The signal transduction process between hepatocyte growth factor (HGF) and its receptor (c-Met) has been shown to contribute to OVCA metastasis and progression. Overexpression of HGF and/or c-Met has been associated with poor clinical outcome in OVCA (7, 13, 19). Silencing of c-Met in OVCA cells with small interfering RNA (siRNA) reduced the cancer burden when these cells were injected into nude mice (19). The c-Met inhibitor exhibited significant antiproliferative effects against a panel of human OVCA cell lines (7, 13). Thus the HGF signaling pathway may be a therapeutic target for OVCA treatment. However, the direct effects of HGF and c-Met inhibitor on OVCA cell invasion through an adherent cell layer have not been thoroughly explored. The conventional approach to assessing cancer invasion, that is, use of Boyden chamber-based technology, is primarily for end-point analysis, which provides information on the number of cancer cells that reach the other side of the chamber (7). Temporal information about the invasion process and interactions of OVCA with the underlying adherent cells induced by HGF and counteracted by c-Met inhibitors cannot be determined with use of the conventional approach.

Electric cell-substrate impedance sensing (ECIS) is an in vitro impedance measuring system to quantify the behavior of cells within an adherent cell layer (4, 11). The most common application of ECIS is to monitor cell spreading and barrier function of adherent cells in a monolayer by measuring the time course of changes in impedance with use of AC voltage at a single frequency of 4 kHz. The same approach can be used to monitor the invasion of OVCA cells through an adherent monolayer such as human umbilical vein endothelial cells (HUVECs) (6, 8). The impedance of a cell monolayer can also be measured as a function of AC frequency. By fitting the frequency-dependent impedance data collected over time into a mathematical model (1, 6, 15), we can determine changes in cell-cell junctional resistance (R_b), cell-substrate separation (h), and cell membrane capacitance (C_m) of the monolayer. Monitoring the changes in these cellular biophysical parameters will reveal the interactions between OVCA cells and the endothelial monolayer during the invasion process. We have been successfully using this approach to detect the time-dependent changes of R_b, h, and C_m of the HUVEC monolayer (15).

The aim of this study is to investigate the effects of HGF and a c-Met inhibitor (SU11274) on human OVCA transendothelial invasion in real time by monitoring the changes in impedance with single-frequency mode and multiple-frequency scan mode. The present study demonstrated the successful use of ECIS to monitor OVCA cell invasion (SKOV-3 cells) through the HUVEC monolayer in real time, which revealed the temporal information of invasion and alteration in biophysical

Address for reprint requests and other correspondence: K.-P.Yip, Dept. of Molecular Pharmacology and Physiology, Morsani College of Medicine, Univ. of South Florida, MDC 8, 12901 Bruce B. Downs Blvd., Tampa, FL 33612 (e-mail: dyip@health.usf.edu).

parameters associated with the cancer cells and the underlying adherent cells.

MATERIALS AND METHODS

Cell culture. Human SKOV-3 OVCA cells and HUVECs were used for invasion studies. SKOV-3 is not a high-grade serous OVCA cell line (3), but it had been used previously in ECIS measurement (18, 20). SKOV-3 cells (ATCC, Manassas, VA) were grown in M199 and MCDB 105 medium (1:1) (Sigma, St. Louis, MO) supplemented with 10% fetal calf serum, 2 mM L-glutamine, 100 units/ml penicillin, and 100 μg/ml streptomycin. SKOV-3 cells were subcultured when they reached 80% confluency. HUVECs (Cambrex, Walkersville, MD) were maintained in endothelial cell growth medium (Cambrex) supplemented with 10 ng/ml human recombinant epidermal growth factor, 1 μg/ml hydrocortisone, 50 μg/ml gentamicin, 50 ng/ml amphotericin B, 12 μg/ml bovine brain extract, and 2% fetal bovine serum. HUVECs were subcultured when they reached 70% confluency. Only HUVECs with less than six passages were used in the experiments. All cells were grown in cell culture flasks before seeding into ECIS electrode wells. All cells in flasks and in ECIS electrode wells were maintained in a humidified atmosphere with 5% CO_2 at 37 °C.

Impedance measurement and detection of cellular micromotion. To study cell behavior via ECIS, cells were grown in cell culture wells with gold electrodes embedded on the bottom (Applied BioPhysics, Troy, NY). Culture medium was used as the electrolyte. Each well contained a small working electrode (area ~5 × 10^{-4} cm^2) and a large counter electrode (area ~0.15 cm^2). Cells were seeded with a density of 1 × 10^5 cells/cm^2 in each well. An AC voltage at 4 kHz of 1 μÅ was applied between working and counter electrodes, while the voltage was monitored with a lock-in amplifier. Both in-phase and out-of-phase voltage data were stored and processed with a computer (11). Electrode arrays, relay bank, lock-in amplifier, and software for the ECIS measurement were from Applied BioPhysics. For detection of cellular micromotion, impedance data of each well were collected at 1 Hz for 2,048 s. The time-series data were then normalized. The variance of each time series was calculated as described previously (12, 15).

Frequency-dependent impedance and cellular biophysical parameters. The impedance of the cell-electrode system was measured as a function of frequency ranging from 25 Hz to 60 kHz. The frequency scan measurement in each well required 150 s to complete. Frequency-dependent impedance was first determined in each well (electrode) without cells. Cells were seeded with a density of 1 × 10^5 cells/cm^2 in each well. Frequency-dependent impedance of the confluent cell layer was then monitored in individual wells under various combinations of experimental conditions. To acquire the time course of changes in frequency-dependent impedance in some experiments, a frequency scan of impedance was repeated every hour up to 20 h. The R_b, h, and C_m of the cell layer and the effective radius of spread cell (r_c) were determined by fitting the frequency-dependent impedance into a cell-electrode mathematical model for circular disk-shaped cells (4, 10, 11).

Intracellular Ca^{2+} concentration measurement in OVCA cells. SKOV-3 OVCA cells grown on a collagen-coated glass bottom culture dish were loaded with fluo-4/AM (10 μM; Invitrogen, Carlsbad, CA) in Hanks' balanced salt solution for 30 min, followed by 20 min for deesterification (9, 14). Fluo-4 was excited at 488 nm, and the

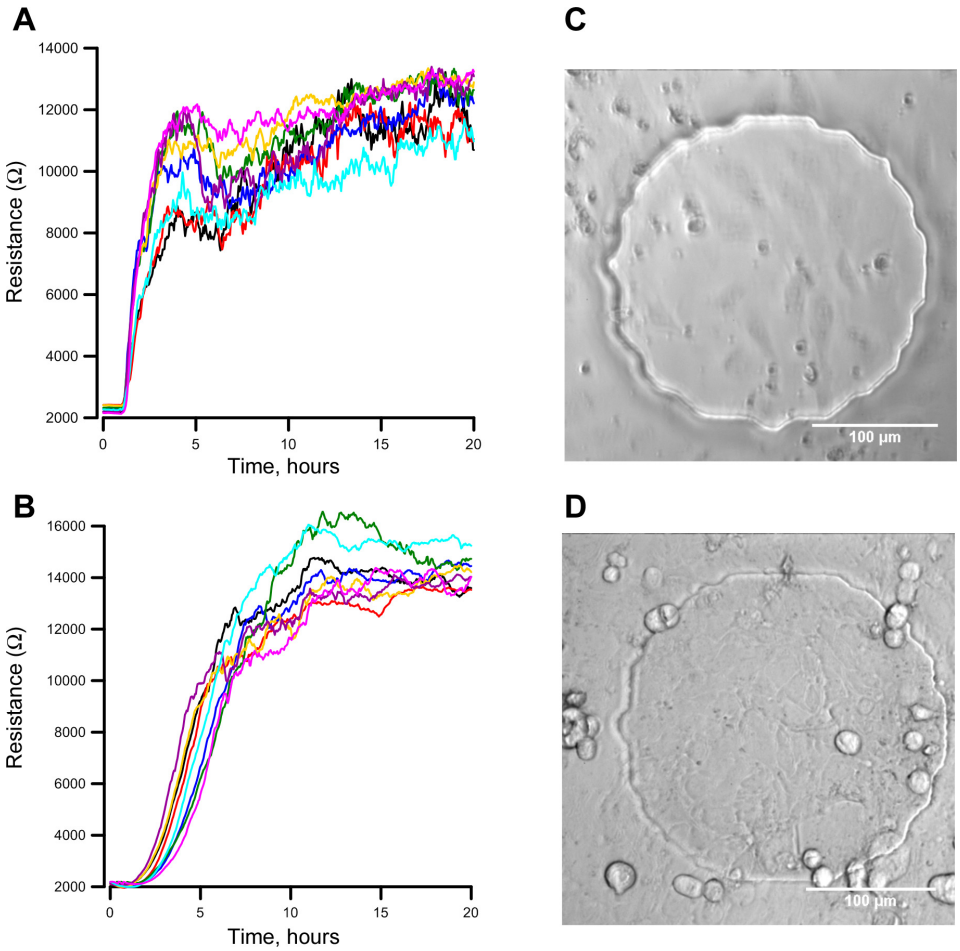

Fig. 1. Time courses of change in resistance due to the attachment and spreading of HUVECs (*A*) and SKOV-3 cells (*B*) in eight different electrode-containing wells in the same array. Images of confluent layer of HUVECs (*C*) and SKOV-3 cells (*D*) on the ECIS electrode wells were taken 20 h after cell seeding. The circular area is the gold electrode, which is 250 μm in diameter. Each colored line represents the time course from a single electrode-containing well. Scale bar is 100 μm in length.

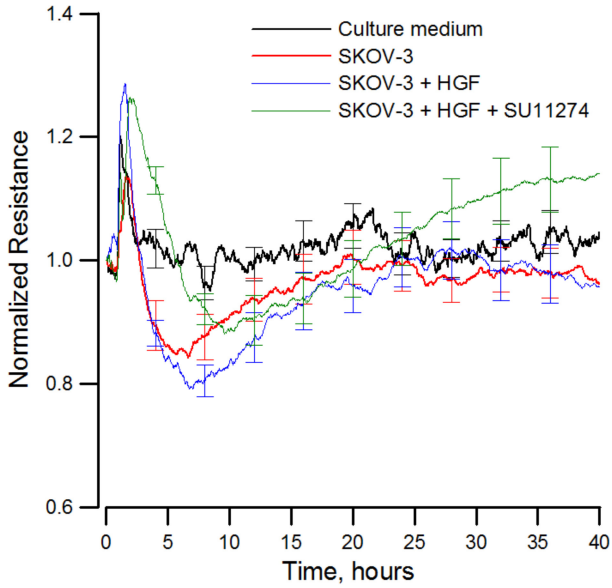

Fig. 2. Normalized time course of resistance changes in the HUVEC monolayers induced by SKOV-3 cells in the presence and absence of HGF (50 ng/ml) and c-Met inhibitor SU11274 (5 μM). SKOV-3 cell suspension was added to the top HUVEC monolayer at a ratio of 1:1 at 1 h. Each colored line indicates a different experimental condition (n = 8). The measured resistance was normalized by the value at the start of each run.

emission was collected with a spectral window of 495–540 nm at 0.25 Hz with a Leica TCS SP5 confocal imaging system. Temporal variations of intracellular Ca^{2+} concentration ($[Ca^{2+}]_i$) in individual cells were measured from stored images with Leica Application Suite Advanced Fluorescence software.

Data analysis. Results were reported as means ± SE. The number (n) was the number of replicate wells from at least four independent experiments unless indicated otherwise. Statistical significance was calculated by using the Student t-test for paired or unpaired data. Analysis of variance of regression coefficient (slope of the regression line) was used to compare time-dependent changes in R_b, h, and C_m. All time course data from the same experimental condition were normalized and fitted with the least square method to a straight line (BMDP statistical package, Program 1R).

RESULTS

Cell attachment and spreading. Impedance is a complex number composed of a real number and an imaginary unit. Resistance is the real number part of impedance. Figure 1*A* shows the time course of changing resistance after HUVECs were seeded on gelatin-coated electrodes. Eight individual culture wells were used to monitor the changes in impedance (resistance) from *time 0* before the cells were seeded to 20 h after cell layers were confluent. The data were collected with an AC voltage of 4 kHz. The cell-free resistance was about 2 kΩ in each well. After HUVECs were seeded into the electrode-containing wells, the initial increase in resistance was the result of cell attachment. This observation likely resulted from the fact that the insulating plasma membranes of cells effectively blocked the area available for current flow and caused the current to flow beneath and between the cells. The measured resistance value peaked at 12 h and reached ~9~12 kΩ when cell spreading was completed. The fluctuations observed in the resistance curves were due to the spontaneous cellular micromotion. Figure 1*C* shows the confluent HUVEC layer at 20 h after cell seeding into the electrode-containing well. Figure 1*B* shows the attachment and spreading of SKOV-3 cells. The resistance value of SKOV-3 cells consistently reached 13~14 kΩ within about 10 h after cell seeding, indicating that SKOV-3 cells attached and spread well on the electrode, as shown in Fig. 1*D*.

Time course of SKOV-3 cells transendothelial extravasation. Figure 2 shows the time course of changes in normalized electrical resistance of the HUVEC confluent layer challenged by adding SKOV-3 cells to the top HUVEC monolayer for up to 40 h. The initial transient in every time course was due to the addition of cancer cells and/or medium. The time course of the control (black line) without the addition of SKOV-3 cells was very steady after the initial transient, as expected, since there were no cancer cells invading into the endothelial monolayer. SKOV-3 cell invasion manifested as a rapid decrease in resistance as SKOV-3 cells infiltrated into the HUVEC monolayer and compromised the barrier function of the HUVECs (red line), which reached the lowest point after 5 h of exposure to SKOV-3 cells. This rapid decrease in resistance was potentiated in the presence of HGF (blue line) in terms of both duration and magnitude. The lowest resistance was reached after 7 h of exposure to SKOV-3 cells. The potentiation induced by HGF was attenuated in the presence of a c-Met inhibitor (green line).

Cellular biophysical parameters derived from frequency-dependent impedance. Impedance of the cell layer was measured as a function of AC frequency from 25 Hz to 60 kHz. The R_b, h, and C_m were then calculated based on a mathematical model (6, 15). Table 1 shows the analysis of frequency-dependent impedance of HUVECs and SKOV-3 cells on the ECIS electrode at 20 h after cell seeding. R_b, h, and C_m values were shown for HUVECs and SKOV-3 cells. The effective radius for the spread cell (parameter required in the mathematical model) was measured and determined to be 20 μm for HUVECs and 15 μm for SKOV-3 cells. R_b of SKOV-3 cells was three times higher than that of HUVECs, and h of SKOV-3 cells was only one-fifth of that found in HUVECs. However, C_m of SKOV-3 cells was comparable to that of HUVECs.

Table 1. *Impedance analysis of frequency-scan data obtained from confluent HUVEC and SKOV-3 cell layers cultured on ECIS electrodes 20 h after cell seeding*

	R_b, Ω·cm^2	h, nm	C_m, μF/cm^2
HUVEC (r_c = 20 μm)	2.1 ± 0.1 (n = 337)	107 ± 3 (n = 337)	2.5 ± 0.1 (n = 337)
SKOV-3 (r_c = 15 μm)	7.7 ± 0.5* (n = 32)	22.8 ± 2.5* (n = 32)	2.3 ± 0.2 (n = 32)

Values are means ± SE. The effective radius for the spread cell (r_c), the junctional resistance between cells (R_b), the average cell-substrate separation (h), and the specific membrane capacitance (C_m) were calculated by comparing the measured impedance spectra with the calculated values obtained from the electric cell-substrate impedance sensing (ECIS) cell-electrode model. *Difference is significant ($P < 0.05$) when compared with the same parameter of human umbilical vein endothelial cells (HUVECs).

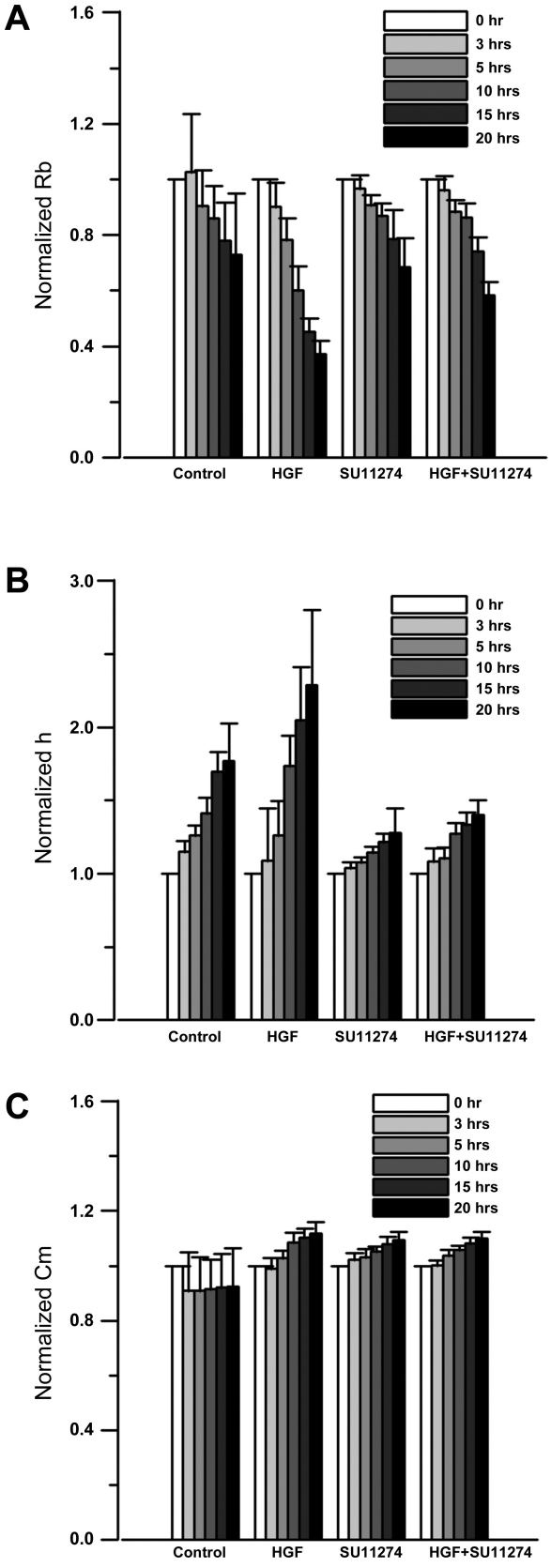

Effect of HGF on SKOV-3 cell morphology and motility. The effects of HGF and c-Met inhibitor on SKOV-3 cells in terms of R_b, h, and C_m were examined during the first 20 h of exposure. Frequency-dependent impedance was measured every hour for 20 h. Three hours of incubation of HGF or c-Met inhibitor did not alter the R_b or h (Fig. 3). However, 20 h of HGF incubation reduced the R_b in SKOV-3 cells by almost 50% (Fig. 3*A*) compared with the timed control. The HGF-induced decrease in R_b was abolished in the presence of c-Met inhibitor. Twenty hours of HGF incubation increased h by ~25% compared with the timed control (Fig. 3*B*), which was abolished in the presence of c-Met inhibitor. Regression analysis of the time course of changes in R_b and h indicated that the decrease in R_b and the increase in h induced by HGF were significant ($P < 0.001$) compared with the timed control (Table 2). Coincubation of a c-Met inhibitor significantly ($P < 0.001$) reduced the effect of HGF to decrease R_b and increase h. The increases in C_m induced by HGF or c-Met inhibitor were less obvious compared with increases in h. In general, there was a trend of increasing C_m when measurements were taken at 20 h than when they were taken at 3 h after incubation (Fig. 3*C*), reflecting the proliferation of cells in culture.

The decrease in junctional resistance and increase of cell-substrate separation suggested HGF triggered mobilization and scattering of SKOV-3 cells. The observations from scratch wound-induced migration of SKOV-3 were consistent with this notion (Fig. 4). The cell migration velocity was increased by ~70% ($P < 0.05$, $n = 10$) in the presence of HGF. The c-Met inhibitor (SU11274) alone did not alter the cell migration but attenuated the cell migration triggered by HGF. HGF also induced intracellular Ca^{2+} mobilization in SKOV-3 cells (Fig. 5). Periodic calcium spikes were frequently observed in individual SKOV-3 cells. The Ca^{2+} mobilization was impaired in the presence of c-Met inhibitor. All of these observations were consistent with the notion that HGF stimulated SKOV-3 motility by interaction with c-Met.

Effect of c-Met inhibitor on HUVEC cell morphology and motility. The c-Met inhibitor SU11274 alone induced a dose-dependent immediate increase in resistance in the HUVEC monolayer, which decayed slowly during the 40-h recording period (Fig. 6*A*). The corresponding values of R_b, h, and C_m after 40 h of SU11274 exposure are shown in Table 3 and suggested that SU11274 enhanced the function of the HUVEC monolayer barrier by increasing R_b and decreasing h in a dose-dependent manner. However, there were no significant changes in C_m. In contrast, the introduction of SKOV-3 cells to the top of the HUVEC monolayer triggered a decrease in transendothelial resistance, which suggested the invasion of SKOV-3 cells into the HUVEC monolayer (Fig. 6*B*). The attenuation of SKOV-3 invasion was SU11274 dose-dependent. In the absence of HGF, SU11274 (>3 μM) abolished the decrease in transendothelial resistance (cancer cell invasion). The corresponding values of R_b and h after 40 h of SU11274

Fig. 3. Changes in cellular biophysical parameters of confluent SKOV-3 cell layers upon challenge with 50 ng/ml HGF, 5 μM SU11274, and HGF + SU11274, respectively. Normalized junctional resistance (*A*), average cell-substrate separation (*B*), and membrane capacitance (*C*) of the SKOV-3 cell layers were obtained through analysis of frequency-dependent impedance. Results are means ± SE ($n = 4$).

Table 2. *Regression analysis of time-dependent changes in R_b, h, and C_m in SKOV-3 cell layer induced by HGF and c-Met inhibitor SU11274*

	R_b		h		C_m	
	Intercept	Regression coefficeint, h^{-1}	Intercept	Regression coefficeint, h^{-1}	Intercept	Regression coefficeint, h^{-1}
Control	1.02	−0.016 ± 0.004	0.99	0.043 ± 0.004	0.94	−0.002 ± 0.003
HGF	0.96	−0.034 ± 0.002*	0.94	0.073 ± 0.009*	0.99	0.007 ± 0.001*
SU11274	1.02	−0.016 ± 0.002	1.00	0.014 ± 0.002*	0.92	0.005 ± 0.001*
HGF + SU11274	1.02	−0.020 ± 0.001†	1.01	0.021 ± 0.002*†	0.98	0.005 ± 0.001*

Values are means ± SE; $n = 4$. The same data set in Fig. 3 was used for the ANOVA of regression coefficient over groups. Data of each experimental condition were fitted with the least square method into a straight line using data collected every hour for 20 h. R_b, junctional resistance between cells; h, the average cell-substrate separation; C_m, specific membrane capacitance; HGF, hepatocyte growth factor. *The regression line was significantly different ($P < 0.001$) when compared with the regression line of the control. †The regression line was significantly different ($P < 0.001$) when compared with the regression line of HGF.

exposure are shown in Table 3 and suggest that SU11274 at high doses (>3 μM) increased the R_b and reduced the h of the HUVEC monolayer, even in the presence of SKOV-3 OVCA cells. The C_m was reduced by 10% in the presence of SKOV-3 cells. Since the maximal decrease in transendothelial resistance was found at about 5 h after exposure to cancer cells, the effects of HGF and SU11272 on the cellular micromotion of SKOV-3 after 5 h of exposure were investigated (Table 4). HGF decreased the junctional resistance and increased the cellular micromotion of the SKOV-3 monolayer, which were counteracted by SU11274. These observations were consistent with the notion that HGF increased SKOV-3 cell motility via c-Met.

DISCUSSION

The present study successfully implemented the use of ECIS to monitor the invasion of SKOV-3 cells into the HUVEC monolayer and demonstrated that the changes in biophysical parameters of SKOV-3 cells and HUVECs were modulated by HGF and c-Met inhibitor SU11274 in the invasion process. Determining the changes in these parameters was achieved by measuring the changes in impedance with 4 kHz AC to monitor cancer cell invasion and by measuring impedance as a function of AC frequency (25 Hz to 60 KHz) to monitor the changes in cellular biophysical parameters. The junctional resistance between the cells (R_b), the average cell-substrate separation (h), and membrane capacitance (C_m) were estimated based on the experimentally determined frequency-dependent impedance and a mathematical model (6, 15).

ECIS measurement of transendothelial invasion of cancer cells has several advantages over other cancer invasion measurements. First, the ECIS assay can provide information about the temporal interactions between cancer cells and endothelial cell layer during the invasion. Invasion of SKOV-3 cells into the HUVEC monolayer occurred in the first 5 h (Fig. 2). HGF prolonged the invasion phase, increased the drop of transendothelial resistance, and slowed down the recovery phase of transendothelial resistance. c-Met inhibitor attenuated the effects of HGF in all these three aspects of transendothelial invasion. Second, the ECIS assay can reveal changes in biophysical cellular parameters in cancer cells (SKOV-3) and endothelial cells (HUVECs) induced by the invasion stimulant (HGF) and invasion retardant (SU11274). HGF increased the motility of SKOV-3 cells as indicated by the decrease in R_b, the increase in h, and the increase in cellular micromotion. C-met inhibitor counteracted the effects of HGF in R_b, h, and micromotion (Fig. 3 and Table 4). Exposing HUVECs to SU11274 did not induce noticeable detrimental effects in HUVEC barrier function (decrease in transendothelial resistance); instead, SU11274 enhanced the transendothelial resistance of the HUVEC monolayer (Fig. 6*A*). Thus the ECIS approach to monitor cancer invasion provides not only temporal information on invasion but also the mechanisms of stimulation or inhibition of the invasion process. For the screening of potential therapeutic agents to inhibit transendothelial cancer invasion, one critical criterion is that the selected agent should not be cytotoxic to endothelial cells. Potential cytotoxic effects of c-Met inhibitor on HUVECs can be screened by monitoring of HUVEC spontaneous cellular micromotion, as we previously reported (15). Finally, ECIS follows real-time impedance changes during transendothelial invasion, whereas the other methods are primarily for end-point analysis.

ECIS impedance measurement has also been successfully integrated with Boyden-like chamber preparation to detect the migration of cancer cell through a microporous membrane. However, the increase of the measured impedance in this type of preparation represents the number of penetrating cancer cells that reach the electrode. On the other hand, our newly developed ECIS extravasation assay is based on changes in electrical impedance at the cell/electrode interface. As cancer cells attach and invade through the HUVEC monolayer, the disruption of endothelial junctions, the retraction of endothelial cells, and the replacement of endothelial cells by tumor cells lead to a substantial change in ECIS impedance.

In a previous study, a decrease in transendothelial resistance was described as a means to qualitatively monitor the migration of breast cancer cells through the HUVEC monolayer under the influence of transforming growth factor-β (TGF-β) (8). Breast cancer cells were preincubated with TGF-β for 24 h before being adding to the top of the HUVEC monolayer. A transient decrease in resistance was detected after 8 h of cancer cell challenge. However, this decrease was measured with a single electrode without duplication, and the transendothelial resistance was measured for only 10 h. There was no quantification of the decrease in transendothelial resistance.

Another study to qualitatively monitor the invasion of SKOV-3 cells through the mesothelial monolayer (human mesothelial cell line LP9) by measuring transmesothelial cell resistance had similar limitations (18). The resistance was monitored for 80 h after the mesothelial monolayer was challenged by SKOV-3 cells. A sustained decrease in transmesothelial cell resistance occurred after 50 h of cancer cell chal-

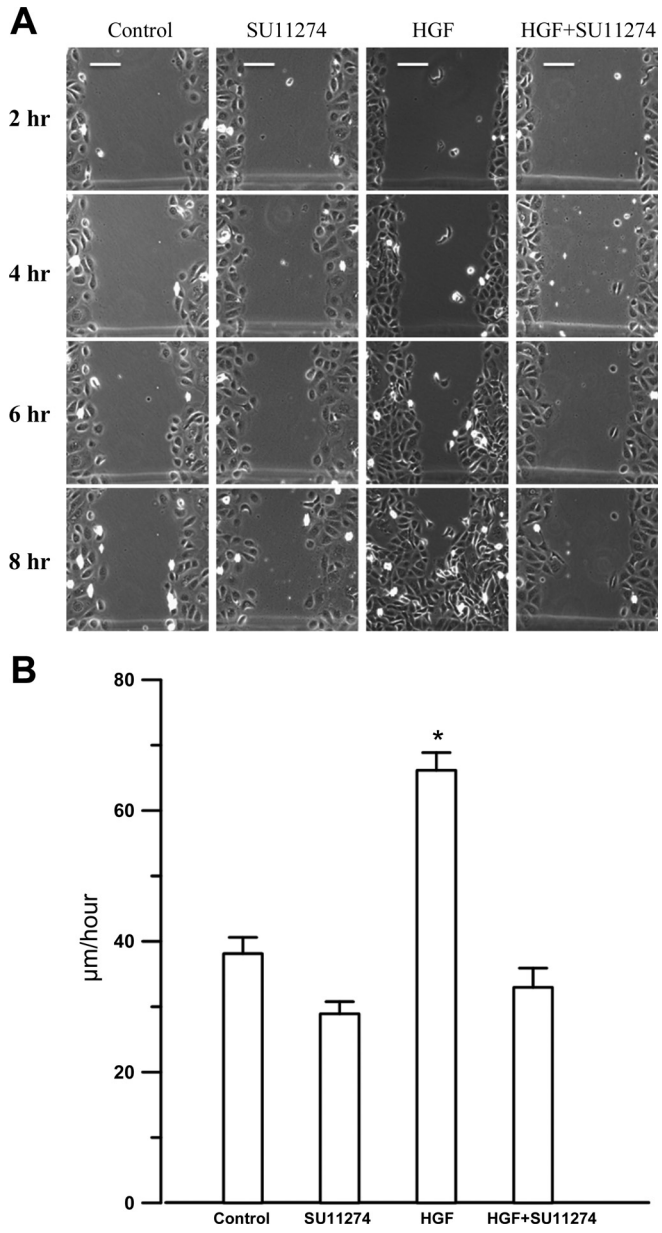

Fig. 4. *A*: time-lapsed images of scratch wound-induced migration of SKOV-3 cells in the control, the presence of c-Met inhibitor SU11274 (5 μM), HGF (50 ng/ml), and HGF + SU11274. Gaps were created by gently dragging a 200-μl pipette tip across the bottom of the 35-mm cultured dishes. *B*: the respective migration rates of SKOV-3 cells over 8 h in the presence of SU11274, HGF, and HGF + SU11274. Results are means ± SE. *Significant difference ($P < 0.05$, $n = 10$) compared with the control. Scale bar is 150 μm in length.

lenge. Although ECIS data were collected with a single electrode (well) in both studies and no quantitative data were presented, these studies did indicate that the invasion of cancer cells was associated with a decrease in electrical resistance of the underlying adherent cells, as was observed in the present study. Scanning electron microscopy showed that SKOV-3 cells induced the formation of gaps in the mesothelial cell monolayer after 6 h of coculture (20). Consistent with our observations, the invasion of SKOV-3 cancer cells into the HUVEC monolayer occurred before 5 h after exposing HUVECs to SKOV-3 cells.

HGF increased the motility of SKOV-3 cells, as indicated by an increase in the junctional resistance between the cells (R_b), an increase in the average cell-substrate separation (h), an increase in cellular micromotion (an increase in the variance in spontaneous fluctuation of electrical resistance), and an increase in migration velocity. All four of these parameters were sensitive to the presence of c-Met inhibitor SU11274, suggesting that interactions between HGF and c-Met are required to increase SKOV-3 motility. It has been demonstrated that Ca^{2+} mobilization is an integral part of HGF/c-Met signaling in hepatic cells (5). HGF also triggered cytosolic Ca^{2+} mobilization in SKOV-3 cells, which was attenuated by c-Met inhibition. However, HGF-induced Ca^{2+} mobilization might not be exclusively mediated by c-Met. An increase in intracellular Ca^{2+} is known to underlie directed cell migration (2), the increase in cell traction force in OVCA cells (9), and metastasis (17). The recent discovery of hematogenous metastasis of OVCA to the omentum via circulating tumors cells instigated rethinking about the mode of OVCA metastasis (16). Our approach of using two different modes of impedance measurement to monitor OVCA invasion in real time is not limited to the study of extravasation of cancer cells. By replacing HUVECs with mesothelial cells, this approach can be used to study OVCA invasion in the mesothelium of omentum (21). This newly developed approach is also applicable to studying the invasion of other cancer cells through an adherent layer involving various signaling pathways.

In summary, an approach based on the ECIS technique was successfully developed and implemented to monitor SKOV-3 cell invasion through the HUVEC monolayer in real time. We demonstrated that HGF increases the motility of SKOV-3 for transendothelial invasion, which is mediated by c-Met. c-Met inhibitor SU11274 attenuated the stimulatory effect of HGF on SKOV-3 motility and improved the barrier function of the HUVEC monolayer.

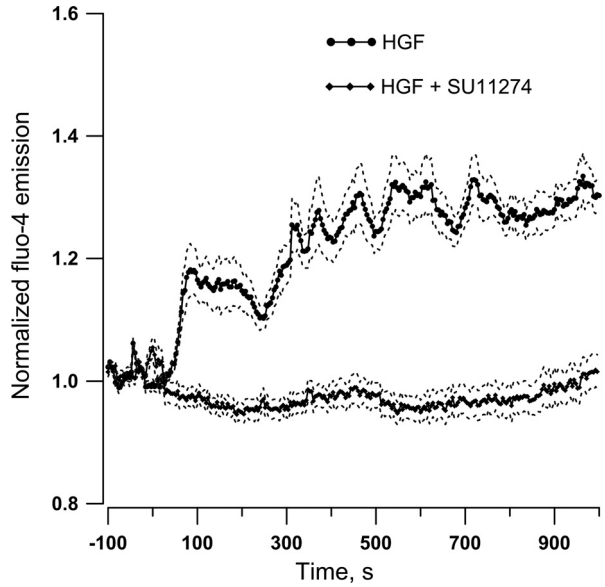

Fig. 5. Normalized time course of calcium mobilization induced by HGF. HGF (50 ng/ml) triggered an immediate increase in intracellular Ca^{2+} (67 cells/3 dishes). Preincubation of SKOV-3 cells with a c-Met inhibitor (SU11274; 5 μM) abolished HGF-induced calcium mobilization (56 cells/3 dishes). HGF was added at time = 0 s. Dotted lines are SE.

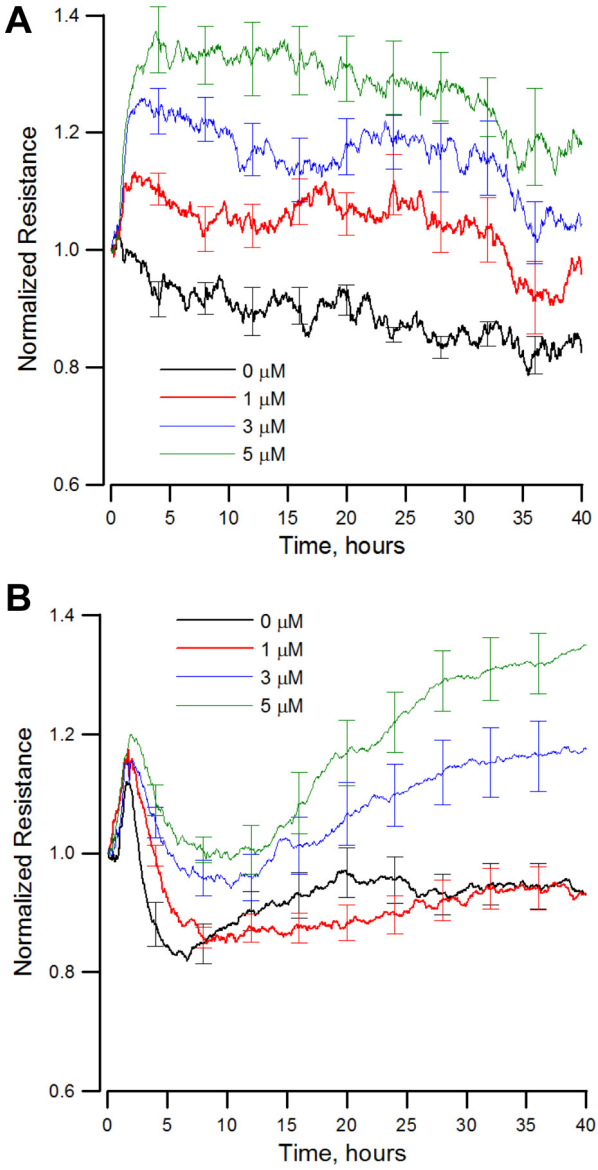

Fig. 6. Normalized time course of resistance changes in HUVEC monolayers incubated with various concentrations of c-Met inhibitor SU11274 in the absence and presence of SKOV-3 cells on top. *A*: HUVECs only ($n = 10$). *B*: HUVECs with SKOV-3 cells on top ($n = 8$). SU11274 and SKOV-3 were added to the HUVEC monolayer at time = 0.5 h. Each colored line indicates a different concentration of SU11274 used. The measured resistance was normalized by the value at the start of each run.

Table 3. *Effect of c-Met inhibitor, SU11274, on the morphological parameters of confluent HUVEC layers 40 h after challenged by SKOV-3 or culture medium (control)*

SU11274	R_b, Ω·cm²	h (nm)	C_m (μF/cm²)
SKOV-3			
Before adding	1.6 ± 0.1 ($n = 63$)	116 ± 5 ($n = 63$)	2.7 ± 0.1 ($n = 63$)
0 μM	1.3 ± 0.2 ($n = 12$)	141 ± 11 ($n = 12$)	2.4 ± 0.1* ($n = 12$)
1 μM	1.2 ± 0.2* ($n = 16$)	122 ± 8* ($n = 16$)	2.4 ± 0.1* ($n = 16$)
3 μM	2.0 ± 0.2* ($n = 18$)	114 ± 5* ($n = 18$)	2.4 ± 0.1* ($n = 18$)
5 μM	2.7 ± 0.2* ($n = 18$)	95 ± 6* ($n = 18$)	2.3 ± 0.1* ($n = 18$)
Control			
Before adding	1.3 ± 0.1 ($n = 21$)	114 ± 5 ($n = 21$)	2.9 ± 0.3 ($n = 21$)
0 μM	1.2 ± 0.1 ($n = 5$)	113 ± 6 ($n = 5$)	3.3 ± 0.4 ($n = 5$)
1 μM	1.3 ± 0.4 ($n = 6$)	107 ± 8 ($n = 6$)	3.5 ± 0.3 ($n = 6$)
3 μM	1.4 ± 0.2 ($n = 7$)	87 ± 8† ($n = 7$)	2.5 ± 0.2 ($n = 7$)
5 μM	1.7 ± 0.4 ($n = 6$)	89 ± 7† ($n = 6$)	3.1 ± 0.4 ($n = 6$)

Values are means ± SE. R_b, junctional resistance between cells; h, the average cell-substrate separation; C_m, specific membrane capacitance. *Difference is significant ($P < 0.05$) when compared with the same parameter before adding SKOV-3 cells. †Difference is significant ($P < 0.05$) when compared with the same parameter before adding medium in control.

GRANTS

This work was supported by the Ministry of Science and Technology of the Republic of China, Taiwan under Contract of MOST102-2628-B-010-010-MY3 (to C.-M. Lo) and National Cancer Institute Grants 1R03-CA-123621-01A1 (to C.-M. Lo), R01-CA-142832 (to K.-P. Yip), and R01-CA-169200 and R01-CA-133057 (to S. C. Mok).

DISCLOSURES

No conflicts of interest, financial or otherwise, are declared by the author(s).

AUTHOR CONTRIBUTIONS

C.-M.L. conceived and designed the research; C.-M.L., J.-C.L., and K.-P.Y. performed experiments; C.-M.L., J.-C.L., P.Y.S., and K.-P.Y. analyzed data; C.-M.L., J.-C.L., P.Y.S., T.-L.Y., S.C.M., and K.-P.Y. interpreted results of experiments; C.-M.L. and K.-P.Y. prepared figures; C.-M.L., P.Y.S., T.-L.Y., S.C.M., and K.-P.Y. drafted manuscript; C.-M.L., P.Y.S., T.-L.Y., S.C.M., and K.-P.Y. edited and revised manuscript; C.-M.L., S.C.M., and K.-P.Y. approved final version of manuscript.

REFERENCES

1. **Balasubramanian L, Yip KP, Hsu TH, Lo CM.** Impedance analysis of renal vascular smooth muscle cells. *Am J Physiol Cell Physiol* 295: C954–C965, 2008.
2. **Brundage RA, Fogarty KE, Tuft RA, Fay FS.** Calcium gradients underlying polarization and chemotaxis of eosinophils. *Science* 254: 703–706, 1991.
3. **Domcke S, Sinha R, Levine DA, Sander C, Schultz N.** Evaluating cell lines as tumour models by comparison of genomic profiles. *Nat Commun* 4: 2126, 2013.
4. **Giaever I, Keese CR.** Micromotion of mammalian cells measured electrically. *Proc Natl Acad Sci USA* 88: 7896–7900, 1991.
5. **Gomes DA, Rodrigues MA, Leite MF, Gomez MV, Varnai P, Balla T, Bennett AM, Nathanson MH.** c-Met must translocate to the nucleus to initiate calcium signals. *J Biol Chem* 283: 4344–4351, 2008.
6. **Keese CR, Bhawe K, Wegener J, Giaever I.** Real-time impedance assay to follow the invasive activities of metastatic cells in culture. *Biotechniques* 33: 842–844, 846, 848–850, 2002.
7. **Koon EC, Ma PC, Salgia R, Welch WR, Christensen JG, Berkowitz RS, Mok SC.** Effect of a c-Met-specific, ATP-competitive small-molecule inhibitor SU11274 on human ovarian carcinoma cell growth, motility, and invasion. *Int J Gynecol Cancer* 18: 976–984, 2008.
8. **Kuo YC, Su CH, Liu CY, Chen TH, Chen CP, Wang HS.** Transforming growth factor-beta induces CD44 cleavage that promotes migration of MDA-MB-435s cells through the up-regulation of membrane type 1-matrix metalloproteinase. *Int J Cancer* 124: 2568–2576, 2009.

Table 4. *ECIS cellular micromotion data obtained from confluent SKOV-3 cell layers 5 h after exposure to 50 ng/ml HGF or/and 5 μM SU11274*

	Resistance, kΩ	Variance, $\times 10^{-6}$
Control	16.2 ± 0.4 ($n = 32$)	2.64 ± 0.44 ($n = 32$)
50 ng/ml HGF	14.2 ± 0.5* ($n = 30$)	4.18 ± 0.54* ($n = 30$)
5 μM SU11274	19.2 ± 1.0* ($n = 6$)	1.99 ± 0.60 ($n = 6$)
HGF + SU11274	15.6 ± 1.2 ($n = 6$)	2.11 ± 0.57 ($n = 6$)

Values are means ± SE. Resistance is the average resistance value of the cell layer over a 2,048-s run. Variance is the statistical variance for the 64-point intervals of the normalized 2,048-s data set. *Difference is significant ($P < 0.05$) when compared with the same parameter of the control.

9. **Leung CS, Yeung TL, Yip KP, Pradeep S, Balasubramanian L, Liu J, Wong KK, Mangala LS, Armaiz-Pena GN, Lopez-Berestein G, Sood AK, Birrer MJ, Mok SC.** Calcium-dependent FAK/CREB/TNNC1 signalling mediates the effect of stromal MFAP5 on ovarian cancer metastatic potential. *Nat Commun* 5: 5092, 2014.
10. **Lo CM, Ferrier J.** Impedance analysis of fibroblastic cell layers measured by electric cell-substrate impedance sensing. *Phys Rev E* 57: 6982–6987, 1998.
11. **Lo CM, Keese CR, Giaever I.** Impedance analysis of MDCK cells measured by electric cell-substrate impedance sensing. *Biophys J* 69: 2800–2807, 1995.
12. **Lo CM, Keese CR, Giaever I.** Monitoring motion of confluent cells in tissue culture. *Exp Cell Res* 204: 102–109, 1993.
13. **Marchion DC, Bicaku E, Xiong Y, Bou Zgheib N, Al Sawah E, Stickles XB, Judson PL, Lopez AS, Cubitt CL, Gonzalez-Bosquet J, Wenham RM, Apte SM, Berglund A, Lancaster JM.** A novel c-Met inhibitor, MK8033, synergizes with carboplatin plus paclitaxel to inhibit ovarian cancer cell growth. *Oncol Rep* 29: 2011–2018, 2013.
14. **Mok SC, Bonome T, Vathipadiekal V, Bell A, Johnson ME, Wong KK, Park DC, Hao K, Yip DK, Donninger H, Ozbun L, Samimi G, Brady J, Randonovich M, Pise-Masison CA, Barrett JC, Wong WH, Welch WR, Berkowitz RS, Birrer MJ.** A gene signature predictive for outcome in advanced ovarian cancer identifies a survival factor: microfibril-associated glycoprotein 2. *Cancer Cell* 16: 521–532, 2009.
15. **Opp D, Wafula B, Lim J, Huang E, Lo JC, Lo CM.** Use of electric cell-substrate impedance sensing to assess in vitro cytotoxicity. *Biosens Bioelectron* 24: 2625–2629, 2009.
16. **Pradeep S, Kim SW, Wu SY, Nishimura M, Chaluvally-Raghavan P, Miyake T, Pecot CV, Kim SJ, Choi HJ, Bischoff FZ, Mayer JA, Huang L, Nick AM, Hall CS, Rodriguez-Aguayo C, Zand B, Dalton HJ, Arumugam T, Lee HJ, Han HD, Cho MS, Rupaimoole R, Mangala LS, Sehgal V, Oh SC, Liu J, Lee JS, Coleman RL, Ram P, Lopez-Berestein G, Fidler IJ, Sood AK.** Hematogenous metastasis of ovarian cancer: rethinking mode of spread. *Cancer Cell* 26: 77–91, 2014.
17. **Prevarskaya N, Skryma R, Shuba Y.** Calcium in tumour metastasis: new roles for known actors. *Nat Rev Cancer* 11: 609–618, 2011.
18. **Ren J, Xiao YJ, Singh LS, Zhao X, Zhao Z, Feng L, Rose TM, Prestwich GD, Xu Y.** Lysophosphatidic acid is constitutively produced by human peritoneal mesothelial cells and enhances adhesion, migration, and invasion of ovarian cancer cells. *Cancer Res* 66: 3006–3014, 2006.
19. **Sawada K, Radjabi AR, Shinomiya N, Kistner E, Kenny H, Becker AR, Turkyilmaz MA, Salgia R, Yamada SD, Vande Woude GF, Tretiakova MS, Lengyel E.** c-Met overexpression is a prognostic factor in ovarian cancer and an effective target for inhibition of peritoneal dissemination and invasion. *Cancer Res* 67: 1670–1679, 2007.
20. **Sriram PS, Mohammed KA, Nasreen N, Hardwick J, Van Horn R, Sanders K, Antony VB.** Adherence of ovarian cancer cells induces pleural mesothelial cell (PMC) permeability. *Oncol Res* 13: 79–85, 2002.
21. **Yeung TL, Leung CS, Yip KP, Au Yeung CL, Wong ST, Mok SC.** Cellular and molecular processes in ovarian cancer metastasis. A review in the theme: cell and molecular processes in cancer metastasis. *Am J Physiol Cell Physiol* 309: C444–C456, 2015.